Japanese Journal of Applied Physics **51** (2012) 10NC30 **REGULAR PAPER**
http://dx.doi.org/**10.1143/JJAP.51.10NC30**

Synthesis and Characterization of Wurtzite Cu_2ZnSnS_4 Nanocrystals

Meng-Huan Jao[1], Hsueh-Chung Liao[1], Ming-Chung Wu[1,2], and Wei-Fang Su[1]*

[1]*Department of Materials Science and Engineering, National Taiwan University, Taipei 106-17, Taiwan*
[2]*Department of Chemical and Materials Engineering, Chang Gung University, Taoyuan 333-02, Taiwan*

Received December 19, 2011; accepted February 11, 2012; published online October 22, 2012

Copper–zinc–tin–chalcogenide (CZTSSe) with earth abundant elements has attracted increasing attention due to large absorption coefficient and band gap of ~1.5 eV which is near the optimum band gap of single-junction photovoltaic devices. In this study, we used commercially available precursors to produce wurtzite Cu_2ZnSnS_4 nanocrystals by simple solvothermal synthesis. Different from the typical kesterite or stannite phases of CZTS, the nanocrystals synthesized in this study are in wurtzite phase with hexagonal crystal cell. The *n*-dodecanethiol was used to control the reactivity of metal ions, leading to the controlled size of CZTS nanoparticle by simply varying the reaction time. Furthermore, the as synthesized CZTS nanocrystals have novel wurtzite crystal structure. As a result, a red shift of absorption band edge between the CZTS nanoparticles with different size was obtained. Our study provides an extending method of CZTS nanocrystal ink preparation awaiting for further photovoltaic device application.

1. Introduction

Solar cells have attracted increasing attention due to the global energy issue. Thin film solar cell is a good candidate because of the large absorption coefficient and good power conversion efficiency (PCE). Among thin film solar cells, the light absorber layer made of $CuIn_xGa_{(1-x)}Se_2$ (CIGS) has been demonstrated to be a promising materials for solar energy conversion, showing high PCE (>20%) and excellent stability.[1,2] However, the usage of $CuIn_xGa_{(1-x)}Se_2$ solar cells encounters the challenge of low availability and toxic of indium and gallium. Hence, a substitute: copper–zinc–tin–chalcogenide (CZTSSe) with earth abundant elements was developed. The CZTS has large absorption coefficient[3,4] and band gap of ~1.5 eV[5] which is near the optimum band gap of single-junction photovoltaic devices.[6] Additionally, the deposition of absorber layer by solution process was recently extensively investigated as an alternative deposition method of co-evaporation.[7,8] Such chemical wet approach benefits from low cost and ease of chemical composition control. Todorov *et al.* reported the fabrication of CZTSSe thin film solar cells with 9.6% PCE using a hydrazine-based solution via spin coating.[9] Hillhouse and Agrawal[10] reported a PCE of 7.2% by depositing nanocrystal dispersion. Namely, chalcopyrite nanoparticles were synthesized with accurate ratio and dispersed in organic solvent as an ink for deposition.

Nanocrystals feature size-dependent properties within the dimension of Bohr exciton radius. Hence it provides an effective strategy to manipulate the optical band gap by tuning the nanocrystal size. Controlling the size of chalcogen-based semiconductor nanoparticle such as PbS, PbSe, CuS, CdS, CdSe, etc. has been extensively studied.[11–17] However, the reports of size control for nanocrystals with ternary or quaternary compounds are still limited.[18] It can be attributed to the difficulties of controlling the reactivity of precursors for three or four elements at the same time. In this study, we used *n*-dodicanethiol as the sulfide precursor to control the reaction with other three metal ions.[19] Size-controlled Cu_2ZnSnS_4 nanoparticles from 7 to 12 nm were synthesized and characterized. Different from the typical kesterite or stannite phases of CZTS, the nanoparticles synthesized in the present study are in wurtzite phase with hexagonal crystal cell.[20] Moreover, shift of the optical band gap resulted from size variation is observed. The present work extends the current technology of nanocrystal synthesis awaiting for further application in thin film solar cells.

2. Experimental Methods

In this work, copper(II) acetate monohydrate (Aldrich, 99.99+%), zinc acetate dihydrate (Acros, 98%), tin(II) acetate (Aldrich, 99.995+%), *n*-dodecanethiol (Aldrich, ≥99.8%), and 1-octadecene (Aldrich, 90%), and sulfur (Acros, 99.999%) were purchased and used as-received without further purification. A mixture of 1 mmole of copper acetate monohydrate, 0.5 mmole of zinc acetate dihydrate, 0.5 mmole of tin acetate, 10 mmole of dodecanethiol, and 10 mL of octadecene were added into a 100 mL three-neck-flask equipped with reflux condenser. The mixture was vigorously stirred under vacuum at 120 °C for 30 min to eliminate moisture. During this step, the solution color changed from light blue to turbid green. Afterward, N_2 was purged into the flask for 30 min. The solution color changed from turbid green to clear yellow. The reaction was then heated up to 240 °C rapidly and kept at 240 °C for four different reaction times, 5, 10, 20, and 40 min respectively. Finally, the reaction was cooled down to room temperature and precipitated out by acetone followed by centrifugation. The supernatant was decanted and the precipitation was dispersed into toluene or chloroform. The process was repeated for several times for removing residue precursor and surfactant. The obtained colloidal nanoparticles were dispersed in toluene. In addition, we also synthesized kesterite CZTS nanocrystals to compare with wurtzite CZTS nanocrystals. For synthesis of kesterite CZTS nanocrystals, 2 mmole elemental sulfur was used as the sulfide precursor dissolved in oleylamine instead of *n*-dodecanethiol dissolved in octadecene. The other synthesis procedure is as same as that of wurtzite CZTS nanocrystals.

The microstructure and elemental analysis of CZTS nanoparticles were studied by transmission electron microscopy (TEM; FEI Tecnai G2 F20, 200 kV) equipped with energy dispersive X-Ray spectrometer (EDX; JEOL JSM6510, 15 kV). The crystalline structures were verified by X-ray diffractonmeter (PANalytical X'Pert PRO). For the optical property of CZTS nanoparticles, various CZTS nanoparticles dispersed in toluene (1.0 mg/mL) and then measured by UV–visible absorption spectroscopy (PerkinElmer Lambda 35).

*E-mail address: suwf@ntu.edu.tw

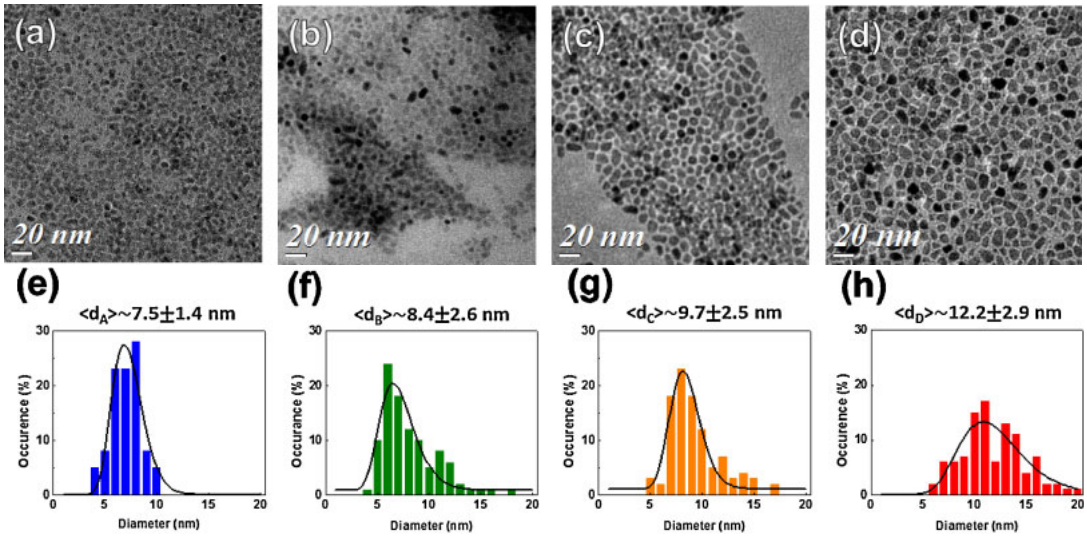

Fig. 1. (Color online) TEM images (a–d) and size distribution (e–h) of CZTS nanoparticles with respective to different reaction time, 5 (a, e), 10 (b, f), 20 (c, g), and 40 min (d, h), respectively.

3. Results and Discussion

In this study, we used *n*-dodecanethiol as sulfur precursor instead of the typically used sulfer powder to balance the reactivity of metal cations. Figures 1(a)–1(d) and 1(e)–1(h) show the TEM images and the particle size distribution respectively, with respective to different reaction time, 5 (a, e), 10 (b, f), 20 (c, g) and 40 min (d, h). It can be observed that the particle size increased from 7.5 ± 1.4 to 8.4 ± 2.6 nm when increasing the reaction time from 5 to 10 min. By further increasing the reaction time to 20 and 40 min, the nanoparticle size gradually grew to 9.7 ± 2.5 and 12.2 ± 2.9 nm, respectively. It indicates that the size of the nanoparticles can be easily tuned by varying the reaction time. In addition, the size distribution also increases with increased reaction time as shown in Figs. 1(e)–1(h). The results suggest that the nucleation process was continuously carried out during early reaction stage. The four samples with different reaction time all had the same TEM diffraction pattern, indicating the only crystal structure (wurtzite structure) obtained in the present study.

Figures 2(a) and 2(b) show the XRD patterns and high resolution TEM images of CZTS nanocrsyatls reacted for 40 min respectively. The XRD patterns are not the typical keterite phase but can be indexed to the patterns of wurtzite phase. Corresponding to the diffraction pattern obtained from HRTEM, the diffraction peaks [Fig. 2(a)] can be identified according the previous literature[20] as indicates in the inset of Fig. 2(b). Moreover, it can be carried out that the lattice constants a and c of the CZTS nanocrystals are 3.81 and 6.28 Å, respectively, which is consistent to the reported literature with $a = 3.83$ Å and $c = 6.33$ Å.[20] The EDX data shown in Fig. 2(c) reveals that the as-synthesis nanoparticles compose of copper, zinc, tin, and sulfur, suggesting that all the metals from the precursors were incorporated into the final product. Additionally, the ratio of four elements, naming Cu, Zn, Sn, and S, are 2.0 : 1.1 : 0.9 : 4.0, are near the target ratio of 2 : 1 : 1 : 4.

The CZTS nanocrystals with different crystal structure can be attributed to the different sulfide precursor and

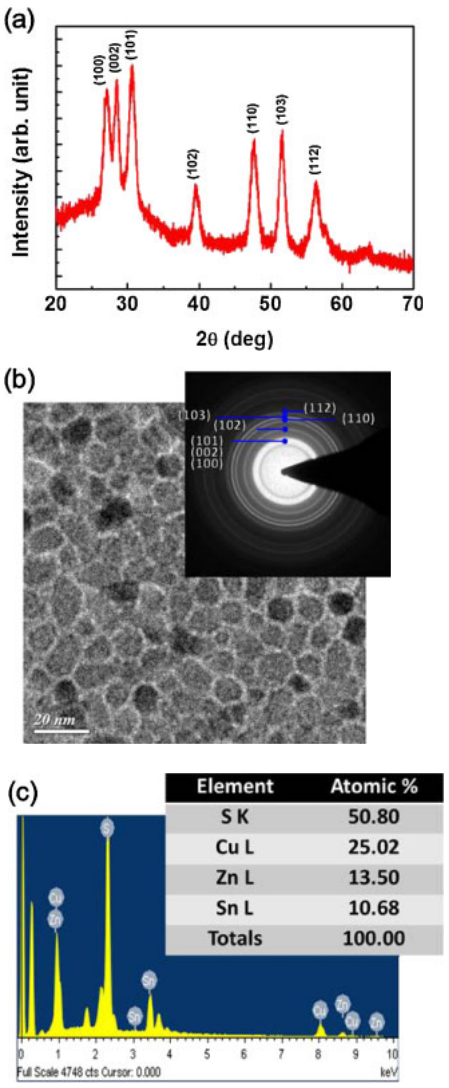

Fig. 2. (Color online) (a) XRD pattern, (b) HRTEM image and diffraction pattern, and (c) EDS analysis of CZTS nanoparticles reacted at 240 °C for 40 min.

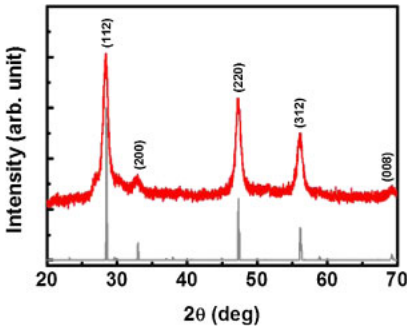

Fig. 3. (Color online) XRD pattern of kesterite CZTS nanoparticles using elemental sulfur as sulfide precursor reacted at 240 °C for 40 min. The red line is the experimental result and the grey line is the data obtained from RRUFF (Ferrokesterite R060870 Powder Diffraction).

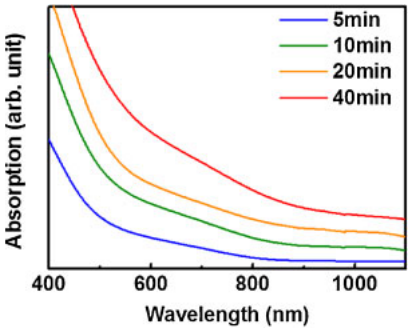

(a)

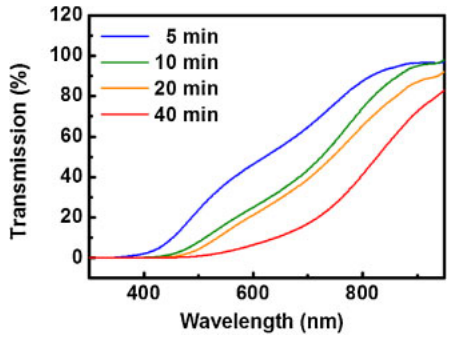

(b)

Fig. 4. (Color online) (a) Absorption spectra and (b) transmission spectra of CZTS nanoparticles reacted for different time.

surface ligand used. In order to prove the precursor effect on the CZTS crystal structure, we also employed elemental sulfur dissolved in oleylamine as sulfide precursor during the synthesis with all the other process remained the same. It can be obtained that the final CZTS nanocrystals exhibit kesterite phase (Fig. 3) which is consistent to the previous literature.[5,10] As a result, the present work demonstrates that the crystal structure of CZTS can be controlled by using different sulfide precursor and surface ligand, i.e., *n*-dodecanethiol in octadecene or sulfur element in oleylamine for wurtzite of kesterite phase respectively.

The absorption and transmission spectra of as-synthesis CZTS nanoparticle with different reaction time are show in Fig. 4. Generally, from both the absorption and transmission spectrum, the obtained wurtzite CZTS nanocrystals harvest the wavelength from UV–vis to near infrared region, which exhibits potential application for further optoelectric application. Additionally, from the absorption spectra it can be observed that no excitonic absorption peaks were observed because the size of the synthesized nanoparticles is much more larger than the Bohr radius of CZTS. Moreover, the inhomogeneous size distribution of the as-synthesis CZTS nanoparticle also leads to unclearly excitonic peaks. However, we can still observe the shift of absorption band edge. Namely, for the nanoparticles reacted for 5 min, the absorption band edge is about 800 nm while the one of nanoparticles reacted for 40 min extends to near 900 nm. The red shift of absorption band edge is due to the size-induced quantum confinement effect. The change in the absorption band edge further indicates the band gap change of CZTS nanoparticles.

4. Summary

In summary, we used commercially available precursors to synthesize Cu_2ZnSnS_4 nanoparticle by simple solvothermal method. The *n*-dodecanethiol was used to control the reactivity of metal ions, leading to the controlled size of CZTS nanoparticle by simply varying the reaction time. Furthermore, the as synthesized CZTS nanoparticles have novel wurtzite crystal structure. As a result, a red shift of absorption band edge between the CZTS nanoparticles with different size was obtained. The present study provides an extending method of nanocrystal ink preparation awaiting for photovoltaic device application.

Acknowledgment

We would like to thank the financial support from National Science Council of Taiwan (NSC 100-3113-E-002-012 and NSC 101-2218-E-182-001) for this research.

1) A. Chirilă, S. Buecheler, F. Pianezzi, P. Bloesch, C. Gretener, A. R. Uhl, C. Fella, L. Kranz, J. Perrenoud, S. Seyrling, R. Verma, S. Nishiwaki, Y. E. Romanyuk, G. Bilger, and A. N. Tiwari: Nat. Mater. **10** (2011) 857.
2) R. N. Bhattacharya, M. A. Contreras, and G. Teeter: Jpn. J. Appl. Phys. **43** (2004) L1475.
3) K. Ito and T. Nakazawa: Jpn. J. Appl. Phys. **27** (1988) 2094.
4) K. Maeda, K. Tanaka, Y. Nakano, and H. Uchiki: Jpn. J. Appl. Phys. **50** (2011) 05FB08.
5) C. Steinhagen, M. G. Panthani, V. Akhavan, B. Goodfellow, B. Koo, and B. A. Korgel: J. Am. Chem. Soc. **131** (2009) 12554.
6) R. W. Miles, G. Zoppi, and I. Forbes: Mater. Today **10** [11] (2007) 20.
7) V. K. Kapur, A. Bansal, P. Le, and O. I. Asensio: Thin Solid Films **431–432** (2003) 53.
8) Y. Zhang, M. Ito, T. Tamura, A. Yamada, and M. Konagai: Jpn. J. Appl. Phys. **50** (2011) 04DP12.
9) T. K. Todorov, K. B. Reuter, and D. B. Mitzi: Adv. Mater. **22** (2010) E156.
10) Q. Guo, G. M. Ford, W.-C. Yang, B. C. Walker, E. A. Stach, H. W. Hillhouse, and R. Agrawal: J. Am. Chem. Soc. **132** (2010) 17384.
11) Z. A. Peng and X. Peng: J. Am. Chem. Soc. **123** (2001) 183.
12) M. A. Hines and G. D. Scholes: Adv. Mater. **15** (2003) 1844.
13) R. D. Schaller, M. A. Petruska, and V. I. Klimov: J. Phys. Chem. B **107** (2003) 13765.
14) J. M. Luther, P. K. Jain, T. Ewers, and A. P. Alivisatos: Nat. Mater. **10** (2011) 361.
15) K. Yu, J. Ouyang, M. B. Zaman, D. Johnston, F. J. Yan, G. Li, C. I. Ratcliffe, D. M. Leek, X. H. Wu, J. Stupak, Z. Jakubek, and D. Whitfiel: J. Phys. Chem. C **113** (2009) 3390.
16) L. Bakueva, I. Gorelikov, S. Musikhin, X. S. Zhao, E. H. Sargent, and E. Kumacheva: Adv. Mater. **16** (2004) 926.
17) J. M. Pietryga, R. D. Schaller, D. Werder, M. H. Stewart, V. I. Klimov, and J. A. Hollingsworth: J. Am. Chem. Soc. **126** (2004) 11752.
18) H. Zhong, Y. Zhou, M. Ye, Y. He, J. Ye, C. He, C. Yang, and Y. Li: Chem. Mater. **20** (2008) 6434.
19) H. Zhong, Z. Wang, E. Bovero, Z. Lu, F. C. J. M. V. Veggel, and G. D. Scholes: J. Phys. Chem. C **115** (2011) 12396.
20) X. Lu, Z. Zhuang, Q. Peng, and Y. Li: Chem. Commun. **47** (2011) 3141.